

Hydrogenation of CO on Cobalt Catalyst in Fischer – Tropsch Synthesis

Mohsen Mansouri¹, Hossein Atashi^{1*}, Ali A. Mirzaei² and Masoud Karimi¹

¹Department of Chemical Engineering, University of Sistan & Baluchestan, Zahedan 98164-161, Iran

²Department of Chemistry, University of Sistan & Baluchestan, Zahedan 98164-161, Iran

Abstract

The kinetic experiments of Fischer–Tropsch synthesis (FTS) over an industrial Co/K catalyst were carried out in a micro-fixed-bed reactor under the conditions as follows: temperature of 483–513 K, pressure of 8 bar, H₂/CO feed ratio of 1–3, and space velocity of 2700–5200 h⁻¹. The optimal amount of catalyst containing 15wt.%Co/10wt.%K/Al₂O₃ was prepared using impregnation procedure. The combined enol/carbide mechanism as the rate-controlling step gives the most plausible kinetic model among the nine different models tested. The activation energies for optimal kinetic model and power law equation were obtained 111.5 kJ/mol and 100 kJ/mol, respectively.

Keywords: Fischer–Tropsch Synthesis; Fixed-bed Reactor; Co/K/Al₂O₃ Catalyst; Kinetic Modeling

Introduction

The process of converting the synthesis gas into liquid fuels (FTS) is a well-known technology. This method is a promising, developing option for environmentally sound production of chemicals and fuels from coal and natural gas. In view of large coal and natural gas reserves and dwindling petroleum reserves worldwide, it is projected to play an ever increasing role in the coming decades [1,2].

Cobalt-based catalysts are the preferred catalysts for hydrocarbon synthesis because of their high FTS activity, selectivity for long-chain paraffins and low activity for the water–gas shift reaction [3]. Cobalt and Iron-based catalysts often contain small amounts of potassium and other metals such as manganese, calcium, zinc, copper and magnesium as promoters to improve their activity and selectivity [4]. Due to its stronger basicity, potassium has a stronger influences on adsorption of reactants (CO and H₂) on the active sites, and leads to improvements in FTS activity, enhancement in selectivity to olefins, suppression of methane formation and a selectivity shift to higher molecular weight products [5,6].

The kinetics of FTS on cobalt catalysts has received significant attention; in fact, several previous studies [7-11] report kinetic data and rate expressions. Reaction orders for H₂ and CO are in the range 0.5 to 2 and -1.0 to +0.65, respectively; activation energies from these studies cover a range 98-103 kJ/mol [11]. The mechanistic kinetic rate expressions for cobalt catalysts are based on the formation of the monomer species as the rate-determining step in the consumption of synthesis gas. Many kinetic equations have been proposed in the literature for various cobalt catalysts, and these have been obtained either empirically (using a power-law rate equation) or to fit a proposed mechanism [8-14].

Our objective was to develop intrinsic rate expressions for the CO conversion to Fischer–Tropsch products over an impregnation cobalt catalyst on the basis of realistic mechanisms. The kinetics of FT reaction was studied and the rate expressions were tested against experimental data that was obtained on the selected catalysts. A model was successfully devised and the kinetics parameters were determined. Also, a power law kinetic equation for the carbon monoxide rate was obtained.

Experiment

Catalyst preparation

The optimal amount of 15wt.%Co/10wt.%K/Al₂O₃ was prepared by impregnation with an aqueous solutions of Co(NO₃)₂·6H₂O and KNO₃ to incipient wetness of γ-Al₂O₃, which had been previously calcined at 400°C for 8 h to remove the surface adsorbed impurities (Brunauer–Emmett–Teller (BET) surface area of 217 m²/g, pore volume of 0.7 cm³/g). The impregnated sample was dried at 110°C for 2 h and calcined in air at 400°C for 8 h (heating rate of 10°C between 110°C and 400°C); the calcined catalyst was reduced in situ (in the fixed bed reactor described below) in pure H₂ at 400°C for 16 h (heating rate of 10°C between 25 and 400°C).

Fixed bed reactor system

A schematic representation of the experimental setup is shown in Figure 1. FTS was carried out in a fixed-bed micro-reactor made of stainless steel with an inner diameter of 12 mm. Three mass flow controllers (Brooks, Model, 5850E) were used to adjust automatically flow rate of the inlet gases comprising CO, H₂ and N₂ (purity of 99.999%). Mixture of CO, H₂ and N₂ was subsequently introduced into the reactor, which was placed inside a tubular furnace (Atbin, Model ATU 150-15). Temperature of the reaction was controlled by a thermocouple inserted into the catalytic bed and visually monitored by a computer. The catalyst was in situ pre-reduced at atmospheric pressure under H₂–N₂ flow (N₂/H₂ = 1, flow rate of each gas = 30 ml/min), at 400°C for 16 h. In each test, 1.0 g catalyst was loaded and the reactor operated about 12 h to ensure steady state operations were attained.

***Corresponding author:** H. Atashi, Department of Chemical Engineering, University of Sistan & Baluchestan, Zahedan 98164-161, Iran, E-mail: atashi.usb@gmail.com

Received November 01, 2011; **Accepted** February 18, 2012; **Published** February 24, 2012

Citation: Mansouri M, Atashi H, Mirzaei AA, Karimi M (2012) Hydrogenation of CO on Cobalt Catalyst in Fischer–Tropsch Synthesis. J Thermodyn Catal 3:113. doi:10.4172/2157-7544.1000113

Copyright: © 2012 Mansouri M, et al. This is an open-access article distributed under the terms of the Creative Commons Attribution License, which permits unrestricted use, distribution, and reproduction in any medium, provided the original author and source are credited.

Catalytic evaluation

Experiments were conducted with mixtures of H₂, CO and nitrogen in a temperature range from 210 to 240°C, H₂/CO feed ratios of 1/1-3/1 (mol/mol) at the pressure of 8 bar. The arrangements of the parameters and the related levels are shown in Table 1. In all of the experiments, the space velocities were between 2700 and 5200 h⁻¹.

To avoid the effect of deactivation, fresh catalysts were loaded in each experiment. To achieve the isothermal conditions in a catalytic bed, the catalyst was diluted with an inert material (quartz). Axial temperature distribution was ensured using Mear’s and Mollavali et al. [15,16] criterion, that is with $L/d_p > 50$. Also, plug-flow was assumed for the gaseous feed. The experimental reaction rate was determined as follows:

$$\text{Rate of conversion of CO} = \frac{(\text{fractional conversion}) \times (\text{input flowrate of CO})}{\text{weight of the catalyst}} \quad (1)$$

Theory

Kinetic expressions

In order to derive rate equations to be adjusted with the data in Table 1, we used Langmuir–Hinshelwood–Houngen–Watson (LHHW) theory to obtain kinetic models. According to this theory, a reaction mechanism should be adopted. Two key assumption of this theory is: (1) Attraction heats are constant, (2) Inherent reaction rates are proportional to surface covers of reactors. To simplify the kinetic models, following assumptions are taken into consideration [17,18]: (1) Presence of an irreversible controlling stage, although all of the other stages are considered to be near the thermodynamic equilibrium. (2)

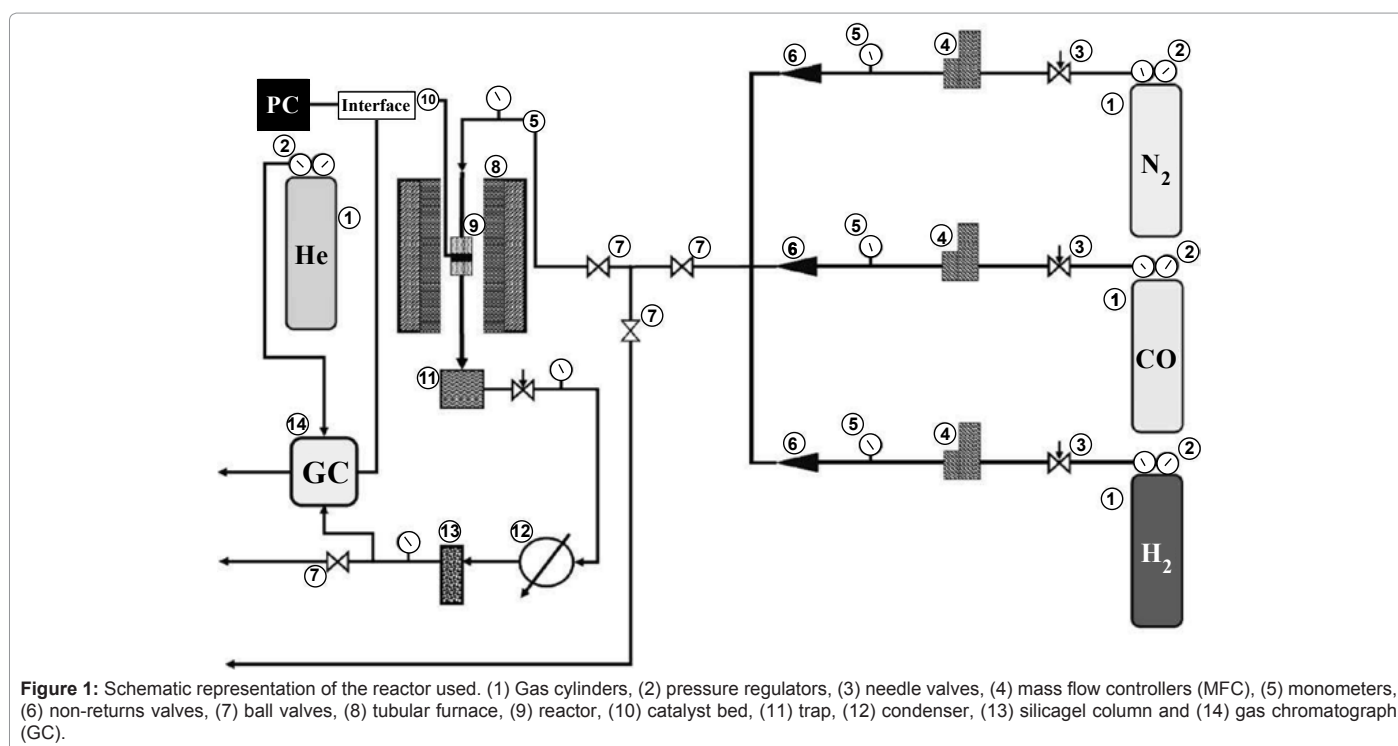


Figure 1: Schematic representation of the reactor used. (1) Gas cylinders, (2) pressure regulators, (3) needle valves, (4) mass flow controllers (MFC), (5) monometers, (6) non-returns valves, (7) ball valves, (8) tubular furnace, (9) reactor, (10) catalyst bed, (11) trap, (12) condenser, (13) silicagel column and (14) gas chromatograph (GC).

Number of data	Temperature (K)	X _{CO} (%)	P _{H₂} (bar)	P _{CO} (bar)	F/W (mol/gr cat. h)	-r _{CO} (mmol/gr cat. h)
1	483.15	2.6	2.81	1.95	0.172	4.471
2	483.15	3.2	2.35	2.90	0.173	5.55
3	483.15	3.6	3.55	1.93	0.154	5.528
4	483.15	4.8	2.25	3.81	0.139	6.659
5	493.15	3.2	3.05	1.94	0.289	9.254
6	493.15	2.4	1.41	1.95	0.195	4.687
7	493.15	5.3	3.33	2.84	0.287	15.20
8	493.15	2.8	2.59	0.97	0.143	4.002
9	503.15	5.1	1.81	1.90	0.186	9.505
10	503.15	7.9	4.73	1.84	0.355	28.01
11	503.15	5.5	3.61	1.42	0.272	14.94
12	503.15	6.7	2.23	2.80	0.286	19.16
13	513.15	8.8	2.88	3.65	0.698	61.42
14	513.15	7.6	3.63	2.31	0.650	49.42
15	513.15	7.1	3.41	1.86	0.520	36.92
16	513.15	8.6	4.58	2.29	0.712	61.22

Table 1: Summary of experimental conditions and results at P = 8 bar and T = 210-240°C.

Concentrations of all of the mediums on the catalyst surface are in steady state. (3) Catalytic locations are steady and distributed homogenously. (4) Throughout the temperature and pressure region, rate controller stage and the most abundant surface medium are remained unchanged. (5) Elementary attraction of hydrogen and carbon monoxide in pseudo-equilibrium state are within concentrations of gaseous phase. (6) Water is removed after the CO decomposition irreversibly.

Statistical criteria using polymath software

Least square method and non-linear regression analysis based on the summarized values in Table 1 was used to determine the power-law equation parameters and kinetic model parameters from experimental data provided in Table 2 using Polymath* software. The software uses Levenberg–Marquardt algorithm to estimate the constants of the model. There are some conditions to find the best model [19]: (1) Obtained constants must be positive. (2) Optimal model or equation is the one which gives the reliable R². (3) Coefficients of the equation must obey Arrhenius and Vanthouff rules. (4) The equation must have the ability to predict the behavior of a differential reactor. A good equation can satisfy all of the mentioned rules. Different statistical indices in Polymath software can be used to determine the quality of regression models and compare them.

Results and Discussion

Development of kinetic equations

Considering the proceeding assumptions, three mechanisms were offered on the basis of various monomer formation (elementary reactions) and carbon chain distribution pathways. An elementary reactions set on sites for each model is summarized in Table 2.

To derive each kinetic model, initially one of the elementary reaction (in some case two or three) steps was assumed as rate-determining step and all other steps were considered at equilibrium. Then, all of the models obtained were fitted separately against the experimental data. In the interest of conciseness, only certain selected kinetic models are reported in the Table 3.

For example derivation of the rate equation for FT-I4 is explained

Model	Number	Elementary Reaction
FT-I	1	CO + s ↔ COs
	2	COs + s ↔ Cs + Os
	3	H ₂ + 2s ↔ 2Hs
	4	Cs + Hs ↔ CHs + s
	5	CHs + Hs ↔ CH ₂ s + s
	6	Os + Hs → HOs + s
	7	HOs + Hs → H ₂ Os + s
	8	H ₂ O + s → H ₂ Os
FT-II	1	CO + s ↔ Cos
	2	H ₂ + 2s ↔ 2Hs
	3	COs + Hs ↔ HCOs + s
	4	HCOs + Hs ↔ Cs + H ₂ Os
	5	Cs + Hs ↔ CHs + s
	6	CHs + Hs ↔ CH ₂ s + s
	7	H ₂ O + s → H ₂ Os
FT-III	1	CO + s ↔ COs
	2	COs + H ₂ ↔ H ₂ COs
	3	H ₂ COs + H ₂ ↔ CH ₂ s + H ₂ O
	4	COs + s ↔ Cs + Os
	5	Cs + Hs ↔ CHs + s
	6	CHs + Hs ↔ CH ₂ s + s
	7	Os + H ₂ → H ₂ Os
	8	H ₂ O + s → H ₂ Os

Table 2: Elementary reactions mechanism set for FTS.

Model of rate controlling	Kinetic equation
FT-I1	$k P_{CO} / (1 + aP_{CO}^{1/2} + bP_{H_2}^{1/2})$
FT-I3	$k P_{H_2} / (1 + aP_{CO}^{1/2} + bP_{H_2}^{1/2})^2$
FT-I4	$k P_{CO}^{1/2} P_{H_2}^{1/2} / (1 + aP_{CO}^{1/2} + bP_{H_2}^{1/2})^2$
FT-I5	$k P_{CO}^{1/2} P_{H_2}^{3/4} / (1 + aP_{CO}^{1/2} P_{H_2}^{-1/4} + bP_{H_2}^{1/2})^2$
FT-II1	$k P_{CO} / (1 + aP_{CO}^{1/2})$
FT-II3	$k P_{CO}^{1/2} P_{H_2} / (1 + aP_{CO}^{1/2})$
FT-III1	$k P_{CO} / (1 + aP_{CO})$
FT-III2	$k P_{CO} P_{H_2} / (1 + aP_{CO})$
FT-III3	$k P_{CO} P_{H_2}^2 / (1 + aP_{CO})$

Table 3: Reaction rate expressions for the FTS, $r_{FT} (\text{mmol g}_{\text{cat}}^{-1} \text{h}^{-1})$.

here. To do this, the first step was considered to be the rate limiting stage and the reaction was irreversible. The remaining steps can be considered to be quick and at equilibrium.

The rate expression of the rate-determining step for FT-I4 model where surface carbon reacts with adsorbed dissociated hydrogen as the rate limiting step, can be expressed irreversible adsorption as follows:

$$-r_{CO} = k_4 \theta_C \theta_H = k_6 \theta_O \theta_H \quad (2)$$

where $-r_{CO}$ is the rate of disappearance of CO, k_4 and k_6 are the forward rate constant for elementary reaction of numbers of 4 and 6 respectively, and θ_i is the surface fraction occupied with adsorbed species i . The fraction of vacant sites, θ_s , can be calculated from the following balance equation:

$$\theta_s + \theta_{CO} + \theta_H + \theta_{H_2CO} + \theta_{CH_2} + \theta_O + \theta_{OH} + \theta_{H_2O} = 1 \quad (3)$$

In this case, it is assumed that adsorbed dissociated hydrogen and surface carbon occupies a significant fraction of the total numbers of sites. Other species were assumed to be negligible in the stoichiometric balance:

$$\theta_s + \theta_C + \theta_H = 1 \quad (4)$$

The surface coverage of carbon monoxide and adsorbed dissociated hydrogen are calculated from the site balance, and the preceding reaction steps which are at quasi-equilibrium:



$$k_1 P_{CO} \theta_s - k_{1,des} \theta_{CO} = 0 \quad (6)$$

$$\theta_{CO} = K_1 P_{CO} \theta_s \quad (7)$$

$$K_1 = \frac{k_1}{k_{1,des}}$$

where K_1 is the equilibrium constant of CO adsorption step. Thus, if the next stages are assumed to be near the thermodynamic equilibrium, available surface ratios can be determined using partial pressures of reactors.

$$\theta_H = K_3^{1/2} P_{H_2}^{1/2} \theta_s \quad (8)$$

$$\theta_o = \frac{k_4}{k_6} \theta_c \quad (9)$$

$$\theta_c = \frac{K_2 \theta_{CO} \theta_s}{\theta_o} \quad (10)$$

Substituting equation (7) and then (9) in equation (10) gives:

$$\theta_c = \frac{K_2 \theta_{CO} \theta_s}{\theta_o} = \left(\frac{K_1 K_2 k_6}{k_4} \right)^{1/2} P_{CO}^{1/2} \theta_s \quad (11)$$

Substituting Equation (8) and (11) into Equation (4), the ratio of free active site can be expressed as:

$$\theta_s = \frac{1}{1 + \left(\frac{K_1 K_2 k_6}{k_4} \right)^{1/2} P_{CO}^{1/2} + K_3^{1/2} P_{H_2}^{1/2}} \quad (12)$$

Substitution of the fraction of vacant sites in Equation (2), the final rate expression is obtained as:

$$-r_{CO} = \frac{(k_4 k_6 K_1 K_2 K_3)^{1/2} P_{CO}^{1/2} P_{H_2}}{\left(1 + \left(\frac{K_1 K_2 k_6}{k_4} \right)^{1/2} P_{CO}^{1/2} + K_3^{1/2} P_{H_2}^{1/2} \right)^2} = \frac{k P_{CO}^{1/2} P_{H_2}}{(1 + a P_{CO}^{1/2} + b P_{H_2}^{1/2})^2} \quad (13)$$

Table 3 summarizes the final form of the different rate expressions for the 9 possible kinetic models considered, whereas Table 4 shows the kinetic and adsorption parameters for the several kinetic models. It can be seen that the pressure dependency of CO and H₂ in the numerator ranges from 1/2 to 1, and 1/2 to 2, respectively. The denominator is quadratic in case of a dual site elementary reaction, in contrast to a single site rate-determining step. The denominator consists of the individual contributions of significantly plentiful species on the catalyst surface.

Also, power law kinetic equation for the carbon monoxide rate was considered for comparison with experimental data. Yang et al.

[8] obtained empirical rate expressions for supported cobalt catalysts using a fixed-bed reactor via regression of a power-law equation of the general form:

$$-r_{CO} = k_0 \exp\left(\frac{-E}{RT}\right) P_{CO}^m P_{H_2}^n \quad (14)$$

Where P_{CO} is the partial pressure of carbon monoxide, k_0 the reaction rate constant, E the activation energy of CO consumption, m the reaction order for CO, and n the reaction order for H₂.

Model parameters and model discrimination

CO consumption rate was obtained from the data in Table 1 using the differential method of data analysis. The kinetic data presented in Table 1 for CO conversion were used for testing the power law equation and nine models listed in Table 3. Before inserting the equations in the Polymath[®] software, Arrhenius and adsorption equations were substituted in kinetics models: Equation (15) and Equation (16) were substituted for k and a , respectively.

$$k = k_0 \exp\left(\frac{-E}{RT}\right) \quad (15)$$

$$a = a_0 \exp\left(\frac{\Delta H}{RT}\right) \quad (16)$$

According to the statistical results obtained by inserting the data and models, the best model can be selected. Based on the kinetic data, the only plausible mechanism was found to be the FT-III model with combined enol/carbide mechanism as the rate-controlling step.

Atashi and Gharehbaghi [20] reported that carbide mechanism was the CO hydrogenation mechanism over Co/TiO₂ catalyst, and indicates that potassium addition causes intermediate to be oxygenated. However, based on statistical information, the best model was found to be FT-III2 that had the less deviation from experimental data. Therefore, the data were best fitted by a LHHW approach by the rate form

$$-r_{CO} = \frac{k_2 K_1 P_{CO} P_{H_2}}{1 + K_1 P_{CO}}$$

where activation energy was obtained to be 111.5 kJ/mol.

The other models were ignored because: (1) calculations of partial regression related to kinetic equation exceed the maximum number of iterations or trial and errors, (2) confidence interval parameter was high when compared with its absolute values, (3) their constants were negative, (4) did not give the responsible R². Figure 2 shows a comparison between the experimental data and predicted results of the FT-III2 model. The solid line in the figure denotes that calculated is equal to the experimental one and dotted lines over and under the solid line represent 11% deviation. The experimental results were found to have a good agreement with the optimal kinetic model showing about 11% deviation.

The data of this study were fitted fairly well by a power law equation in the form of $-r_{CO} = 2.1 \times 10^8 \exp(-1 \times 10^5 / RT) P_{CO}^{-0.45} P_{H_2}^{0.85}$. The R² value was obtained to be 0.99, which shows power law equation was well matched with the experimental data. Table 5 shows the kinetic parameters calculated for the kinetic FT-III2 model and power law equation. The apparent activation energies were 111.5 and 100 kJ/mol which were very close to activation energies reported previously:

Model of rate controlling	k (x) (mmol g ⁻¹ h ⁻¹ bar ^x)	a(x) (bar ^x)	b (x) (bar ^x)
FT-I1	k ₁ (-1)	(k ₆ K ₁ K ₂ /k ₄) ^{1/2} (-1/2)	K ₃ ^{1/4} (-1/2)
FT-I3	k ₃ (-1)	(k ₆ K ₁ K ₂ /k ₄) ^{1/2} (-1/2)	K ₃ ^{1/4} (-1/2)
FT-I4	(k ₄ k ₆ K ₁ K ₂ K ₃) ^{1/2} (-1)	(k ₄ K ₁ K ₂ /k ₆) ^{1/2} (-1)	K ₃ ^{1/4} (-1/2)
FT-I5	(k ₃ k ₆ K ₁ K ₂ K ₄) ^{1/2} K ₃ ^{1/4} (-5/4)	(k ₆ K ₁ K ₂ /k ₃ K ₄) ^{1/2} K ₃ ^{-1/4} (-1/4)	K ₃ ^{1/4} (-1/2)
FT-II1	k ₁ (-1)	(K ₁ K ₂ K ₄ /k ₃) ^{1/2} (-1/2)	
FT-II3	(k ₃ k ₄ K ₁ K ₂) ^{1/2} (-3/2)	(K ₁ K ₂ K ₄ /k ₃) ^{1/2} (-1/2)	
FT-III1	k ₁ (-1)	K ₁ (-1)	
FT-III2	k ₂ K ₁ (-2)	K ₁ (-1)	
FT-III3	k ₂ K ₁ K ₂ (-3)	K ₁ (-1)	

Table 4: Parameters for the FT kinetic models.

Equation	k ₀ (mol.g Cat ⁻¹ .h ⁻¹ .bar ^x)	E(kJ/mol)	a ₀ (bar ^{-0.5})	ΔH(kJ/mol)	m(-)	n(-)
^a FT-III2	1.01 × 10 ¹¹	111.5	163.2	- 5.26		
^b Power law	2.1 × 10 ⁸	100			-0.45	0.85

x: a = - 2, b = - 0.4

Table 5: Values of the kinetic parameters, activation energy and heat of adsorption of CO with various equations.

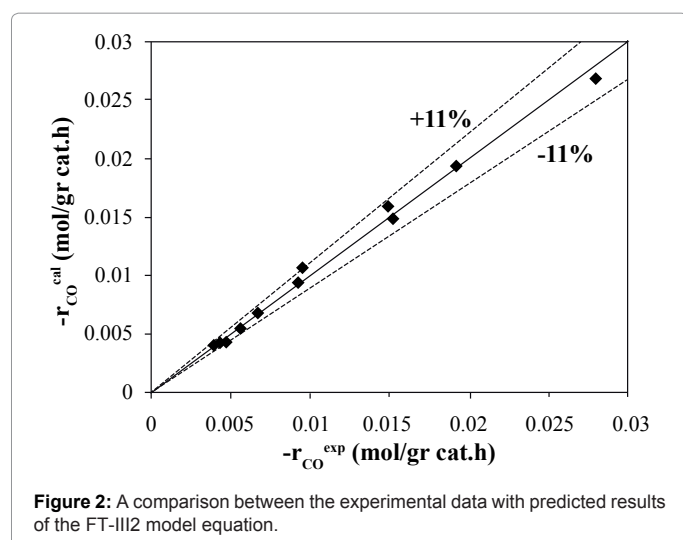


Figure 2: A comparison between the experimental data with predicted results of the FT-III2 model equation.

100 and 103 kJ/mol reported by Yang et al. [8] and Storch et al. [21], respectively. Nevertheless, it was substantially lower than the value of 142 kJ/mol reported by Reuel and Bartholomew [22]. However, Reuel and Bartholomew's value was obtained at significantly lower reactant partial pressure and was based on only two data points, while in this study it was based on sixteen data points.

The reaction orders of 0.85 and -0.45 for H_2 and Co obtained in this study (power law equation) were consistent with those reported in previous kinetic studies of FTS on supported cobalt [8,12,13]. Reaction orders from these studies for H_2 and Co were in the range 0.68 to 1 and -0.24 to -0.5 , respectively.

Conclusion

The optimal amount of catalyst containing 15wt.%Co/10wt.%K/Al₂O₃ was prepared using impregnation procedure. Experiments for the kinetics of the hydrocarbon formation over a cobalt catalyst were obtained over a wide range of industrially relevant reaction conditions. The data of this study were best fitted by the simple LHHW approach by the rate form $-r_{CO} = \frac{k P_{CO} P_{H_2}}{1 + a P_{CO}}$. The values of kinetic constants were obtained and the activation energy was found to be 111.5 kJ/mol for the best model. The data were fitted fairly well by a power law equation in the form of $-r_{CO} = 2.1 \times 10^8 \exp(-1 \times 10^5 / RT) P_{CO}^{-0.45} P_{H_2}^{0.85}$.

References

- Mills GA (1994) Status and future opportunities for conversion of synthesis gas to liquid fuels. Fuel 73: 1243-1279.
- Iglesia E (1997) Design, synthesis, and use of cobalt-based Fischer–Tropsch synthesis catalysts. Appl Catal A: Gen 161: 59-78.
- Lihong S, Debao L, Bo H, Yuhan S (2007) Organic modification of SiO₂ and its influence on the properties of Co-based catalysts for Fischer–Tropsch synthesis. Chin J Catal 28: 999-1002.
- Pour AN, Shahri Smk, Bozorgzadeh HR, Zamani Y, Tavasoli A, et al. (2008) Effect of Mg, La and Ca promoters on the structure and catalytic behavior of iron-based catalysts in Fischer-Tropsch synthesis. Appl Catal A: Gen 348: 201-208.
- Yang Y, Xiang H-W, Xu Y-Y, Bai L, Li Y-W (2004) Effect of potassium promoter on precipitated iron-manganese catalyst for Fischer-Tropsch synthesis. Appl Catal A: Gen 266: 181-194.
- Raje AP, Brien RJO, Davis BH (1998) Effect of potassium promotion on iron-based catalysts for Fischer-Tropsch synthesis. J Catal 180: 36-43.
- Brötz WZ (1949) Zur Systematik der Fischer-Tropsch-Katalyse. Zeitschrift für Elektrochemie 5: 301-306.
- Yang CH, Massoth FE, Oblad AG (1979) Kinetics of CO + H₂ reaction over Co-Cu-Al₂O₃ catalyst. Adv Chem Ser 178: 35-46.
- Sarup B, Wojciechowski BW (1989) Studies of the Fischer-Tropsch Synthesis on a Cobalt Catalyst. II. kinetics of carbon monoxide conversion to methane and to higher hydrocarbons. Can J Chem Eng 67: 62-74.
- Wojciechowski BW (1988) The kinetics of the Fischer-Tropsch synthesis. Catal Rev Sci Eng 30: 629-702.
- Yates IC, Satterfield CN (1991) Intrinsic kinetics of the Fischer-Tropsch synthesis on a cobalt catalyst. Energy Fuels 5: 168-173.
- Wang J (1987) PhD Thesis, Physical, chemical and catalytic properties of borided cobalt Fischer-Tropsch catalysts. Brigham Young University, Provo, UT, USA.
- Zennaro R, Tagliabue M, Bartholomew CH (2000) Kinetics of Fischer-Tropsch synthesis on titania-supported cobalt. Catal Today 58: 309-319.
- Jager B, Espinoza R (1995) Advances in low temperature Fischer–Tropsch synthesis. Catal Today 23: 17-28.
- Mears DE (1974) In Chemical Reaction Engineering II, HM Hulburt Ed., ACS Monograph: Washington 5-11.
- Mollavali M, Yaripour F, Atashi H, Sahebdehfar S (2008) Intrinsic Kinetics Study of Dimethyl Ether Synthesis from Methanol on γ -Al₂O₃ Catalysts. Ind Eng Chem Res 47: 3265-3273.
- Graaf GH, Winkelman JGM, Stamhuis EJ, Beenackers AACM (1988) Kinetics of the three phase methanol synthesis. Chem Eng Sci 43: 2161-2168.
- Van der Laan GP, Beenackers AACM (2000) Intrinsic kinetics of the gas-solid Fischer-Tropsch and water gas shift reactions over a precipitated iron catalyst. Appl catal A: Gen 193: 39-53.
- Bercic G, Levec J (1992) Intrinsic and global reaction of methanol dehydration over γ -Al₂O₃ pellets. Ind Eng Chem Res 31: 1035-1040.
- Atashi H, Gharehbaghi H (2011) Study of CO hydrogenation reaction on cobalt titania catalyst. J Chem Soc Pak 33: 7-11.
- Storch HH, Golumbic N, Anderson RB (1951) The Fischer-Tropsch and Related Syntheses. Wiley, New York, USA.
- Reuel RC, Bartholomew CH (1984) Effects of support and dispersion on the CO hydrogenation activity/selectivity properties of cobalt. J Catal 85: 78-88.